

# An Error Probability Analysis of the Optimum Noncoherent Multiuser Detector for Multipath and Multiantenna Diversity Communications Over Rayleigh-Fading Channels

Artur Russ and Mahesh K. Varanasi, *Senior Member, IEEE*

**Abstract**—The optimum noncoherent multiuser detector is obtained for generalized diversity symbol-synchronous communication systems that employ nonorthogonal multipulse modulation. A unified approach is adopted to simultaneously address various forms of diversity such as time, frequency, multipath, and/or receiver-antenna diversity. Upper and lower bounds on the average bit-error probability of the optimum noncoherent detector are derived. While these bounds are numerically computable, they are too complicated to give insights about the relative influence of system parameters on the essential behavior of the bit-error rate. To address this issue, an asymptotic (low noise) analysis of the bit-error probability is undertaken. It is shown that the upper and lower bounds are indeed asymptotically convergent. A formula for the asymptotic efficiency of the optimum noncoherent detector is thereby derived. Interestingly, the asymptotic efficiency is found to be positive, and independent of the signal strengths of the interfering users.

**Index Terms**—Antenna diversity, code-division multiple-access, error analysis, frequency-selective Rayleigh fading, multipath diversity, multiuser detection, noncoherent detection, nonlinear modulation.

## I. INTRODUCTION

NONORTHOGONAL multipulse modulation (NMM) is considered for wireless multiuser diversity communication systems. In such a scheme, each user transmits  $\log_2 S$  bits of information at a time by sending one of  $S$  possibly nonorthogonal signals. NMM is therefore a generalization of orthogonal multipulse modulation (OMM), a common example of which is frequency-shift keying (FSK). In contrast to quadrature amplitude modulation (QAM) and coherent detection, where joint channel estimation and data detection must be performed (cf. [1], [2]), the problem of signal reception for NMM can be accomplished *noncoherently*, and hence, without

explicit channel estimation. NMM with noncoherent detection is, therefore, the modulation detection method of choice for communications systems that must be designed to operate in severely fading channels where the channel changes too quickly to be reliably estimated, and/or in systems where the extra cost and complexity of channel estimation is undesirable.

In this paper, we consider the generalized diversity Rayleigh fading (GDRF) channel model (see also [3]). The key feature of the GDRF model is that it provides a common framework under which a variety of diversity communication systems that employ time, frequency, multipath, and/or receiver antenna diversity can be studied in a unified manner. Additionally, our GDRF model also allows nonidentical diversity branches with inter-branch signal and fading correlations. Such correlations arise in systems that employ *diversity with discipline*, where no resource (space, time, bandwidth) is used as if it is freely available (cf. [3]). For example, space limitations preclude a sufficient separation of the antennas to yield independent fading across the diversity branches [4].

We consider a multiuser communication system, where several users transmit information simultaneously using NMM and some form of diversity transmission (wideband signaling or time/frequency diversity). Each antenna at the receiver observes a symbol-synchronous superposition of all the active users' transmissions after they have passed through their respective, and possibly frequency-selective, Rayleigh-fading channels. Not only can each user's signal set be nonorthogonal, but we also allow for correlation (intentional or otherwise) between the signal sets of different users. Interuser correlations exist in code-division multiple-access (CDMA) systems, but even in wireless time-division multiple-access (TDMA) and frequency-division multiple-access (FDMA) systems, interuser interference can arise due to intercell interference caused by frequency reuse.

The focus of this paper is on obtaining the fundamental performance limits of noncoherent detection over multiuser GDRF channels. We obtain the optimum noncoherent multiuser detector and analytically study the limiting behavior of its error probability for binary modulation in the high signal-to-noise ratio (SNR) regime (as noise power  $\rightarrow 0$ ).

References to past work in optimum multiuser detection are as follows. An in-depth study of the optimum coherent multiuser detector for the Gaussian channel can be found in [5] and

Paper approved by J. Wang, the Editor for Equalization of the IEEE Communications Society. Manuscript received May 9, 2000; revised June 6, 2001 and September 12, 2001. This work was supported in part by the National Science Foundation under Grant NCR-9725778 and in part by the Army Research Office under Grant DADD19-99-1-0291. This paper was presented in part at the IEEE International Conference on Universal Personal Communications, Florence, Italy, October 1998.

A. Russ was with the University of Colorado, Boulder, CO 80309 USA. He is now with the BMW Group, Munich 81735, Germany.

M. K. Varanasi is with the Department of Electrical and Computer Engineering, University of Colorado, Boulder, CO 80309 USA.

Digital Object Identifier 10.1109/TCOMM.2002.805277

[6]. The same detector is analyzed for the single-path Rayleigh-fading channel in [7]. A joint approach to channel estimation and optimum multiuser detection can be found in [1]. The optimum differentially coherent multiuser detector for differential phase-shift keying (DPSK) modulation was obtained, and its error rate was characterized in [8]. Finally, the optimum noncoherent detector for NMM is obtained and analyzed for the non-diversity Rayleigh-fading channel by the authors of this paper in [9].

The rest of this paper is organized as follows. In Section II, we introduce the system model for generalized diversity communications that employ NMM over a possibly frequency-selective Rayleigh-fading channel. In Section III-A, we obtain the optimum noncoherent multiuser detector for that model when there are multiple receive antennae. In Section III-B, we obtain upper and lower bounds on the error probability of the optimum detector. Section IV contains an asymptotic error rate analysis for the case of binary modulation. A formula for the asymptotic efficiency is also obtained. In Section V, we present examples that illustrate the key results of our analytical work. Section VI concludes the paper.

## II. GENERALIZED DIVERSITY COMMUNICATION SYSTEM MODEL

A mathematical model that yields a unified description of a variety of diversity methods was proposed in [3] in the context of single-user communications and single-pulse modulation. In this section, we extend that model to include multiple users and multipulse modulation. The most important feature of such a model is that it allows us to simultaneously study various forms of multiuser diversity communications in a unified framework.

We limit the development of the diversity model to the case of binary modulation. The extension to  $S$ -ary modulation is straightforward. Let the vector of complex baseband signaling waveforms corresponding to the  $l$ th symbol of user  $k$  in the  $L_w$  “waveform diversity” channels be defined as

$$\mathbf{s}_{kl}(t) = [s_{kl}(t, 0), s_{kl}(t, 1), \dots, s_{kl}(t, L_w - 1)]^T. \quad (1)$$

In the case of time diversity, these waveforms are nonzero in nonoverlapping time intervals, which in turn are usually chosen to be sufficiently separated, so that the different waveforms experience independent fading. In frequency diversity, they are transmitted simultaneously in time ( $t$  denotes the time in the interval  $[0, T]$  for the zeroth symbol interval), but are separated sufficiently in frequency for the same reason. In multipath diversity, a single wideband waveform of bandwidth  $W$  (wideband relative to the coherence bandwidth  $\Delta f_c$  of the channel) is transmitted, and in this case, the channel is frequency selective, and admits an equivalent tapped delay line model [10]. The receiver effectively observes a linear combination of  $L_w$  time-translates of the signal, translated by integer multiples of  $1/W$ , and where  $L_w$  is the integer part of the ratio  $W/\Delta f_c$ . Hence,  $\mathbf{s}_{kl}(t) = [s_{kl}(t)s_{kl}(t - 1/W), \dots, s_{kl}(t - (L_w - 1)/W)]^T$ . In this form of diversity, it is commonly assumed that the transmitted signal is of sufficient bandwidth so that its time translates are orthogonal [10]. Note also that the signals are nonzero over the interval

$[0, T + (L_w - 1)/W]$ , thereby causing intersymbol interference (ISI). We, however, assume that the multipath spread is small compared to the symbol duration, so that ISI occurs over a small fraction of the symbol duration.

In our generalized diversity model, we allow for the possibility that the resources of time, space, or bandwidth are not freely available, and hence, that the  $L_w$  waveforms in (1) are not orthogonal, nor are the fading coefficients associated with them independent. We will, without loss of generality, let each of the  $L_w$  waveforms be normalized to unit energy.

In order to give a succinct model for the received signal, we introduce the following notation. Let  $\mathbf{s}_k(t, i)$  be a two-dimensional (2-D) ( $S$ -dimensional in  $S$ -ary modulation) column vector consisting of the two signals of the  $i$ th waveform diversity channel of user  $k$ , so that  $\mathbf{s}_k(t, i) = (s_{k1}(t, i), s_{k2}(t, i))^T$ , and form the  $2 \times L$  matrix  $\mathbf{S}_k(t)$  as

$$\begin{aligned} \mathbf{S}_k(t) &= [\mathbf{s}_k(t, 0), \mathbf{s}_k(t, 1), \dots, \mathbf{s}_k(t, L_w - 1)] \\ &= \begin{bmatrix} \mathbf{s}_{k1}^T(t) \\ \mathbf{s}_{k2}^T(t) \end{bmatrix}. \end{aligned} \quad (2)$$

Let  $\mathbf{c}_k(m) = (c_{k0}(m), c_{k1}(m), \dots, c_{k(L_w-1)}(m))^T$  be a vector of complex fading coefficients associated with the  $L_w$  waveform diversity channels of user  $k$  and the  $m$ th receiver antenna ( $1 \leq m \leq M$ ). We assume that the fading coefficients  $\mathbf{c}_k(m)$  are essentially constant over the duration of one symbol interval, but they are allowed to vary arbitrarily from one symbol interval to another. It is in this sense that we describe the channel under consideration as exhibiting severe fading. In this work, we focus on Rayleigh fading so that the fading coefficients are complex, zero-mean, Gaussian random variables. We allow the fading coefficients  $\{\mathbf{c}_k(m)\}_{m=1}^M$  associated with each user over all antennas to be mutually correlated (but require that the  $ML_w$ -dimensional covariance matrix of these coefficients is full rank for each  $k$ ). However, these fading coefficients are assumed to be mutually statistically independent between different users. Finally, we let the 2-D vector  $\boldsymbol{\kappa}_k$  denote the signal that is transmitted by user  $k$  with  $\boldsymbol{\kappa}_k \in \{(1, 0)^T, (0, 1)^T\}$ .

The low-pass representation of the signal part  $h_{k,m}(t)$  of the received signal at antenna  $m$  when user  $k$  transmits in isolation can be written as

$$\begin{aligned} h_{k,m}(t) &= \sqrt{E_k} \sum_{i=0}^{L_w-1} c_{ki}(m) \mathbf{s}_k^T(t, i) \boldsymbol{\kappa}_k \\ &= \sqrt{E_k} [\mathbf{S}_k^T(t) \boldsymbol{\kappa}_k]^T \mathbf{c}_k(m). \end{aligned} \quad (3)$$

If  $K$  users transmit information simultaneously, the received signal at antenna  $m$ , which now consists of  $K$  signal components, each having  $L_w$  waveform diversity signals, and the additive white Gaussian noise (AWGN)  $z_m(t)$  (with variance  $\sigma^2$ ), can be succinctly written as

$$r_m(t) = \boldsymbol{\kappa}^T \mathbf{E}^{1/2} \mathbf{C}^T(m) \mathbf{s}(t) + z_m(t) \quad (4)$$

where  $\boldsymbol{\kappa}$  is the  $2K \times 1$ -dimensional vector obtained by stacking the  $K$  2-D vectors  $\boldsymbol{\kappa}_k$  for  $k = 1, \dots, K$  in that order, and  $\mathbf{E}^{1/2}$  is a  $2K \times 2K$ -dimensional diagonal matrix containing the square roots of the energies of the  $K$  users (each repeated twice along

the diagonal). The  $2L_w K \times 2K$ -dimensional block diagonal matrix  $\mathbf{C}(m)$  is defined as

$$\mathbf{C}(m) \triangleq \begin{pmatrix} \mathbf{c}_1(m) & \mathbf{0} & \mathbf{0} & \dots & \mathbf{0} \\ \mathbf{0} & \mathbf{c}_1(m) & \mathbf{0} & \dots & \mathbf{0} \\ \mathbf{0} & \mathbf{0} & \mathbf{c}_2(m) & \dots & \mathbf{0} \\ \vdots & \vdots & \vdots & \ddots & \vdots \\ \mathbf{0} & \mathbf{0} & \mathbf{0} & \dots & \mathbf{c}_K(m) \end{pmatrix} \quad (5)$$

where the  $\mathbf{0}$ 's are  $L_w$ -dimensional column vectors. Finally, the  $2L_w K$ -dimensional column vector  $\mathbf{s}(t)$  is obtained by stacking the  $2K$ ,  $L_w$ -length signal vectors  $\mathbf{s}_{11}(t), \mathbf{s}_{12}(t), \dots, \mathbf{s}_{K1}(t), \mathbf{s}_{K2}(t)$ . The AWGN processes  $\{z_m(t)\}_{m=1}^M$  are assumed to be mutually independent.

Next, we obtain an equivalent discrete-time model for the diversity channel. In describing the signaling scheme of this paper, we assumed that each waveform is confined to a time interval of length  $T$ . If the channel is frequency selective, however, there is a time overlap of adjacent symbol intervals. In single-user spread-spectrum communications, this ISI is usually neglected [10], because the symbol duration is much longer than the multipath spread. In multiuser communications, however, the frequency selectivity not only results in ISI but also in interuser intersymbol interference (IU-ISI). The latter effect could lead to a severe deterioration of the system performance in near-far conditions. Hence, we proceed by masking out the received signal over time intervals with IU-ISI, as proposed in [11]. The masking of the time intervals  $[iT, iT + (L_w - 1)/W]$  can be easily accomplished by multiplying the received signal by a periodic binary waveform which is zero for the above-mentioned time intervals, and one everywhere else.

After passing the received signal through this IU-ISI mask, an obvious way to obtain the sufficient statistics at each receive antenna would be to employ a bank of matched filters matched to each of the  $2K$  signaling waveforms and their  $L_w$  time translates, which would require  $2L_w K$  matched filters and samplers. In the case of frequency-selective fading, a more efficient method requires only one matched filter per signaling waveform (cf. [11]) per receive antenna. The outputs corresponding to the  $l$ th signal of user  $k$  are stored in the  $L_w$ -dimensional vector  $\mathbf{y}_{kl}$ .

This kind of processing is performed for all  $2K$  signaling waveforms, which results in the  $2L_w K$ -dimensional vector  $\mathbf{y}_m$ , whose dependence on the transmitted symbols can be written as

$$\mathbf{y}_m = \sigma^{-1} \int_{\mathcal{T}} r_m(t) \mathbf{s}^*(t) dt = \mathbf{R} \mathbf{C}(m) \mathbf{\Omega}^{1/2} \boldsymbol{\kappa} + \mathbf{n}_m \quad (6)$$

where  $\mathbf{\Omega} = \sigma^{-2} \mathbf{E}$ , and where the  $2L_w K \times 2L_w K$ -dimensional signal correlation matrix  $\mathbf{R}$  is defined as

$$\begin{aligned} \mathbf{R} &= \int_{\mathcal{T}} \mathbf{s}^*(t) \mathbf{s}^T(t) dt \\ &= \begin{pmatrix} \mathbf{R}_{11} & \mathbf{R}_{12} & \dots & \mathbf{R}_{1\ 2K} \\ \mathbf{R}_{21} & \mathbf{R}_{22} & \dots & \mathbf{R}_{2\ 2K} \\ \vdots & \vdots & \ddots & \vdots \\ \mathbf{R}_{2K\ 1} & \mathbf{R}_{2K\ 2} & \dots & \mathbf{R}_{2K\ 2K} \end{pmatrix}. \end{aligned} \quad (7)$$

Each of the  $L_w \times L_w$  submatrices are defined for  $m, n \in \{1, 2\}$  and  $k, l \in \{1, 2, \dots, K\}$  through

$$\mathbf{R}_{2k-2+m, 2l-2+n} = \int_{\mathcal{T}} \mathbf{s}_{km}^*(t) \mathbf{s}_{ln}^T(t) dt. \quad (8)$$

The additive noise vector  $\mathbf{n}_s$  is Gaussian with zero-mean and covariance matrix  $\mathbf{R}$ .

It remains to normalize the received signal in (3) so that the sum of the energies of the signals  $h_{k,m}(t)$  over the  $M$  receiver antennas is equal to  $E_k$ . Hence, the total average energy of user  $k$  is defined as

$$E_k \triangleq \sum_{m=1}^M E \left[ \int_{\mathcal{T}} |h_{k,m}(t)|^2 dt \right]. \quad (9)$$

$\mathcal{T}$  denotes the symbol duration  $[0, T]$  in time or frequency diversity, and the interval  $[(L_w - 1)/W, T]$  in the case of multipath diversity. The normalization in (9) imposes a constraint on the covariance matrices of  $\mathbf{c}_k(m)$  and on the correlation matrix of the signals of user  $k$ . After substituting (3) into (9), and manipulating the resulting terms, we arrive at the following constraint:

$$\frac{1}{2} \sum_{m=1}^M \text{tr} ((\mathbf{R}_{2k-1, 2k-1} + \mathbf{R}_{2k, 2k}) \boldsymbol{\Sigma}_{kk}(m, m)) = 1 \quad (10)$$

where  $\text{tr}$  stands for the trace of a matrix, and  $\boldsymbol{\Sigma}_{kk}(m, m)$  is the  $L_w$ -dimensional covariance matrix of  $\mathbf{c}_k(m)$  of user  $k$ .

Note that the special case of the model in (6) for a single receive antenna ( $M = 1$ ) is a generalization of the nondiversity model considered in [9].

### III. NONCOHERENT MULTIUSER DETECTION AND MINIMUM ERROR PROBABILITY

We derive the optimum noncoherent multiuser detector and provide upper and lower bounds on its bit-error probability. In so doing, it is not assumed that the channel fading parameters are available at the receiver. The much milder assumption is made, however, that the per-symbol statistics, i.e., the covariance matrices of the per-symbol fading parameters of each user are known.

#### A. Optimum Noncoherent Multiuser Detector

We derive the noncoherent multiuser detector that minimizes the error probability that its joint decision for all users would be in error. The emphasis in this section is on obtaining a description of the optimum detector<sup>1</sup> for the generalized diversity model, that parallels, to the extent possible, that of the optimum detector for the nondiversity channel obtained in [9]. Not only does such a description show precisely how transmitter and receiver diversity expand the nondiversity model, but it also enables an asymptotic analysis of the error probability by appropriately extending the analytical methods of [9].

<sup>1</sup>When there is frequency-selective fading, the optimal detector for the continuous-time model would require sequence detection. We mean optimality for the discrete-time observations  $\{\mathbf{y}_s\}$  that are obtained after the near-optimal IU-ISI mask at a front end. Of course, in the case of single-shot transmission, there would be no need for the IU-ISI mask, and the discrete-time model obtained without masking would be a sufficient statistic with the same structure, so that the optimum detector we consider would, in fact, be optimal for the continuous-time model as well.

The problem of interest here is to obtain the optimum detector that observes the sufficient statistics  $\{\mathbf{y}_m\}_{m=1}^M$ , and determines which one of two signals was sent by each of the  $K$  users.

The key to exposing the similarity of the transmit-receive diversity model to that of the transmit-diversity model in (6) is to rearrange the elements of the  $M$ ,  $2L_w K$ -dimensional vectors  $\{\mathbf{y}_m\}$  into one large  $2ML_w K$  vector according to

$$\mathbf{y} = \sum_{m=1}^M \mathbf{y}_m \otimes \mathbf{e}_m \quad (11)$$

where  $\mathbf{e}_m$  is the  $m$ th column of the  $M$ -dimensional identity matrix, and where  $\otimes$  denotes the Kronecker product operation of two matrices [12]. Note that the  $k$ th  $2L_w M$  elements of  $\mathbf{y}$ , denoted  $\mathbf{y}_k$ , correspond to outputs of matched filters associated with the signals of user  $k$ , of which the first (second)  $M$  elements now correspond to the matched filter outputs across the different antennas associated with the first (second) waveform diversity signal of the first signal of user 1, etc.

Similarly, let  $\mathbf{n} \triangleq \sum_{m=1}^M \mathbf{n}_m \otimes \mathbf{e}_m$ . Let us also define the  $L = ML_w$ -dimensional vector of fading coefficients of user  $k$  as  $\mathbf{c}_k \triangleq \sum_{m=1}^M \mathbf{c}_k(m) \otimes \mathbf{e}_m$  for each  $k = 1, \dots, K$ . It can be easily shown that, with  $\Sigma_{kk}(m, p) \triangleq E[\mathbf{c}_k(m)\mathbf{c}_k^\dagger(p)]$ , the correlation matrix of  $\mathbf{c}_k$  is

$$\Sigma_{kk} \triangleq E[\mathbf{c}_k \mathbf{c}_k^\dagger] = \sum_{m=1}^M \sum_{p=1}^M \Sigma_{kk}(m, p) \otimes \mathbf{e}_m \mathbf{e}_p^T. \quad (12)$$

We define the multiantenna version of the fading coefficient matrix in (5) as the  $2ML_w K \times 2K$ -dimensional block diagonal matrix  $\mathbf{C}$  as

$$\mathbf{C} \triangleq \begin{pmatrix} \mathbf{c}_1 & \mathbf{0} & \mathbf{0} & \dots & \mathbf{0} \\ \mathbf{0} & \mathbf{c}_1 & \mathbf{0} & \dots & \mathbf{0} \\ \mathbf{0} & \mathbf{0} & \mathbf{c}_2 & \dots & \mathbf{0} \\ \vdots & \vdots & \vdots & \ddots & \vdots \\ \mathbf{0} & \mathbf{0} & \mathbf{0} & \dots & \mathbf{c}_K \end{pmatrix} \quad (13)$$

where the  $\mathbf{0}$ 's are  $ML_w$ -dimensional column vectors. Moreover, we will see that the multiantenna version of the signal correlation matrix in (7) is  $\mathcal{R} \triangleq \mathbf{R} \otimes \mathbf{I}_M$ , where  $\mathbf{I}_M$  is the identity matrix of dimension  $M$ . Let  $\gamma_k$  denote the SNR  $E_k/\sigma^2$  of user  $k$ .

The dependence of  $\mathbf{y}$  on the transmitted signals can be written, using elementary properties of the Kronecker product operation [12], as

$$\begin{aligned} \mathbf{y} &= \sum_{m=1}^M \mathbf{R}\mathbf{C}(m)\Omega^{1/2}\boldsymbol{\kappa} \otimes \mathbf{e}_m + \sum_{m=1}^M \mathbf{n}_m \otimes \mathbf{e}_m \\ &= (\mathbf{R} \otimes \mathbf{I}_M) \sum_{m=1}^M (\mathbf{C}(m)\Omega^{1/2}\boldsymbol{\kappa} \otimes \mathbf{e}_m) + \mathbf{n} \\ &= \mathcal{R} \begin{bmatrix} \sqrt{\gamma_1}\boldsymbol{\kappa}_1 \otimes \mathbf{c}_1 \otimes \mathbf{e}_m \\ \sqrt{\gamma_2}\boldsymbol{\kappa}_2 \otimes \mathbf{c}_2 \otimes \mathbf{e}_m \\ \vdots \\ \sqrt{\gamma_K}\boldsymbol{\kappa}_K \otimes \mathbf{c}_K \otimes \mathbf{e}_m \end{bmatrix} + \mathbf{n} \\ &= \mathcal{R}\mathcal{C}\Omega^{1/2}\boldsymbol{\kappa} + \mathbf{n}. \end{aligned} \quad (14)$$

It remains to compute the covariance matrix of the noise vector  $\mathbf{n}$ . Using the assumption that the additive noise processes in the different antennas are mutually independent, we have

$$\begin{aligned} E[\mathbf{n}\mathbf{n}^\dagger] &= E\left[\left(\sum_{m=1}^M \mathbf{n}_m \otimes \mathbf{e}_m\right)\left(\sum_{p=1}^M \mathbf{n}_p \otimes \mathbf{e}_p\right)^\dagger\right] \\ &= E\left[\sum_{m=1}^M \sum_{p=1}^M (\mathbf{n}_m \mathbf{n}_p^\dagger) \otimes (\mathbf{e}_m \mathbf{e}_p^\dagger)\right] \\ &= \sum_{m=1}^M \mathbf{R} \otimes \mathbf{e}_m \mathbf{e}_m^\dagger = \mathbf{R} \otimes \mathbf{I}_M = \mathcal{R}. \end{aligned} \quad (15)$$

The special case of no diversity at the transmitter but with multiple receiver antennas corresponds to  $L_w = 1$ . Here, each user transmits over a frequency-nonselctive channel, and our model provides another generalization of the single-antenna model of [9] to the case of multiple receive antennas. Of course, the most general diversity method supported by the model in (14) includes a combination of transmitter and receiver diversity.

The problem of analyzing the optimum detector is easier to describe if we perform the linear transformation  $\mathcal{R}^{-1} = \mathbf{R}^{-1} \otimes \mathbf{I}_M$  on the vector  $\mathbf{y}$  first. Since the fading correlation matrices for each user are full rank, and since we assume that  $\mathcal{R}$  is invertible, or equivalently, that  $\mathbf{R}$  is invertible, we expect that at least for single-user transmission, the total order of diversity is  $L = ML_w$ . We will see later that this indeed is the total order of diversity even in the multiuser channel, i.e., the presence of interferers does not change the order of diversity relative to the single-user case. The resulting vector  $\mathbf{z} = \mathcal{R}^{-1}\mathbf{y}$  is zero-mean Gaussian, with covariance matrix

$$\mathcal{K}_{\mathbf{z}|H_i} = \gamma \mathcal{D}^{H_i} + \mathcal{Q} \quad (16)$$

where  $\gamma \triangleq E_1/\sigma^2$  is the average SNR of user 1, and we define  $\mathcal{Q} = \mathcal{R}^{-1}$ . The superscript  $H_i$  denotes the  $i$ th hypothesis (there being  $2^K$  hypotheses) and encodes the dependence of the matrix  $\mathcal{D}^{H_i}$  on the particular signals transmitted by the  $K$  users. Furthermore, we define the  $K$ -dimensional vector  $\mathbf{b}$ , with  $b_k \in \{1, -1\}$ , where  $b_k = 1$  ( $b_k = -1$ ) means that the  $k$ th user employs its first (second) signal. Specific realizations of  $\mathbf{b}$  (there are  $2^K$  of them) are denoted through the index  $i$  of  $H_i$ , the  $i$ th hypothesis. We also use the notation  $\mathbf{b}(H_i)$  to express the realization of  $\mathbf{b}$  corresponding to  $H_i$ . This dual representation ( $\mathbf{b}$  and  $H_i$ ) is convenient to characterize the problem at hand. The  $2LK \times 2LK$ -dimensional matrix  $\mathcal{D}^{H_i}$  is block diagonal, with each of its  $L \times L$ -dimensional matrix entries given by

$$\mathbf{D}_{2k-1, 2k-1}^{H_i} = \frac{1}{2} r_k (1 + b_k(H_i)) \Sigma_{kk} \quad (17)$$

$$\mathbf{D}_{2k, 2k}^{H_i} = \frac{1}{2} r_k (1 - b_k(H_i)) \Sigma_{kk} \quad (18)$$

where  $\Sigma_{kk}$  is defined in (12), and  $r_k \triangleq E_k/E_1$  is the ratio of signal energies of user  $k$  and the reference user 1. This notation is convenient to obtain an error rate analysis of user 1 as a function of  $\gamma$  and the energy ratios  $\{r_k\}$  for  $k \in \{2, \dots, K\}$ .

When there are  $K$  active users, each employing two signals, the optimum decision rule, with optimality defined as the minimum probability of erroneous joint decisions, will be a  $2^K$  hy-

potheses testing problem. Assuming equiprobable input signals for each user, the maximum *a posteriori* rule is the maximum-likelihood rule. Consequently, for a given vector  $\mathbf{z}$ , the optimum multiuser detector  $\phi^{\text{opt}}$  selects the hypothesis  $H_i$  according to

$$\hat{i} = \arg \min_{1 \leq i \leq 2^K} \left\{ \mathbf{z}^\dagger \mathcal{K}_{\mathbf{z}|H_i}^{-1} \mathbf{z} + \ln (\det (\mathcal{K}_{\mathbf{z}|H_i})) \right\} \quad (19)$$

where  $\dagger$  denotes the complex-conjugate transpose operation. The extension of (19) to  $M$ -ary nonorthogonal modulation is straightforward, as is the extension to the case where the matrix  $\mathcal{R}$  is not invertible (cf. [9]).

### B. Bounds on Error Probability

Without loss of generality, the performance analysis in this paper is done for the first user. An upper bound on the conditional error probability given  $H_i$  results from invoking a union bound, and a lower bound from considering, just that  $H_j$  which differs only in  $b_1$ , or equivalently, the  $K$ -dimensional error vector  $\mathbf{e}^{ij} = (\pm 1 \ 0 \ 0, \dots, 0)^T$ , with  $\mathbf{e}^{ij}$  defined element-wise as  $e_k^{ij} = 2^{-1}(b_k(H_i) - b_k(H_j))$ . Error vectors which have only one nonzero entry at position one will be of special importance in the asymptotic analysis. We refer to them as unity-weight error vectors.

Let us consider the evaluation of the conditional pair-wise error probability that  $H_j$  gets chosen over  $H_i$  when  $H_i$  is true (henceforth denoted as  $P_{H_i \rightarrow H_j}$ ). It follows from (19) that we must evaluate the probability of the event that the Hermitian quadratic form  $f_{ij} \triangleq \mathbf{z}^\dagger (\mathcal{K}_{\mathbf{z}|H_j}^{-1} - \mathcal{K}_{\mathbf{z}|H_i}^{-1}) \mathbf{z}$  is less than or equal to the real-valued threshold  $c_{ij}$  defined as

$$c_{ij} \triangleq \ln \left( \frac{\det(\mathcal{K}_{\mathbf{z}|H_i})}{\det(\mathcal{K}_{\mathbf{z}|H_j})} \right). \quad (20)$$

Therefore, we obtain the characteristic function [Laplace transform of the probability density function (pdf)] of the Hermitian quadratic form  $f_{ij} = \mathbf{z}^\dagger (\mathcal{K}_{\mathbf{z}|H_j}^{-1} - \mathcal{K}_{\mathbf{z}|H_i}^{-1}) \mathbf{z}$  as being (cf. [13])

$$G_{f_{ij}}(s) = \frac{\prod_{k=1}^N \left( \frac{1}{\lambda_{ij}^k} \right)^{n_k}}{\prod_{k=1}^N \left( \frac{1}{\lambda_{ij}^k} + s \right)^{n_k}} \quad (21)$$

where  $\lambda_{ij}^k$  is the  $k$ th eigenvalue with multiplicity  $n_k$  from the set of  $N$  distinct nonzero eigenvalues of the matrix

$$\mathcal{C}_{H_i H_j} = \mathcal{K}_{\mathbf{z}|H_i} \mathcal{K}_{\mathbf{z}|H_j}^{-1} - \mathcal{I} \quad (22)$$

where  $\mathcal{I}$  is an identity matrix of dimension  $2LK$ . A partial fraction expansion of the characteristic function in (21) yields

$$G_{f_{ij}}(s) = \sum_{k=1}^N \sum_{\nu=1}^{n_k} \frac{A_{k\nu}}{\left( s + \frac{1}{\lambda_{ij}^k} \right)^\nu} \quad (23)$$

where each  $A_{k\nu}$  can be determined from

$$A_{k\nu} = \frac{1}{(n_k - \nu)!} \frac{d^{n_k - \nu}}{ds^{n_k - \nu}} \left[ \frac{\prod_{l=1}^N \left( \frac{1}{\lambda_{ij}^l} \right)^{n_l}}{\prod_{l \neq k}^N \left( \frac{1}{\lambda_{ij}^l} + s \right)^{n_l}} \right]_{s = -1/\lambda_{ij}^k} \quad (24)$$

After an inverse Laplace transform to obtain the pdf, and integrating over appropriate ranges, we obtain for  $c_{ij} \geq 0$  (using the convention that  $0! = 1$ )

$$\begin{aligned} P_{H_i \rightarrow H_j} &= \sum_{\substack{k \\ \lambda_{ij}^k > 0}} \sum_{\nu=1}^{n_k} A_{k\nu} \\ &\times \left[ (\lambda_{ij}^k)^\nu - \sum_{m=0}^{\nu-1} \frac{1}{(\nu-1-m)!} \right. \\ &\quad \left. \times (\lambda_{ij}^k)^{m+1} c_{ij}^{\nu-(m+1)} \exp \left( -\frac{c_{ij}}{\lambda_{ij}^k} \right) \right] \\ &+ \sum_{\substack{k \\ \lambda_{ij}^k < 0}} \sum_{\nu=1}^{n_k} A_{k\nu} (\lambda_{ij}^k)^\nu \end{aligned} \quad (25)$$

and similarly, if  $c_{ij} < 0$ , the corresponding probability becomes

$$\begin{aligned} P_{H_i \rightarrow H_j} &= \sum_{\substack{k \\ \lambda_{ij}^k < 0}} \sum_{\nu=1}^{n_k} A_{k\nu} \exp \\ &\times \left( -\frac{c_{ij}}{\lambda_{ij}^k} \right) \sum_{m=0}^{\nu-1} \frac{1}{(\nu-1-m)!} (\lambda_{ij}^k)^{m+1} c_{ij}^{\nu-(m+1)}. \end{aligned} \quad (26)$$

With this result for each individual conditional error probability, the above-mentioned upper and lower bounds on the overall bit-error probability become

$$P \leq \frac{1}{2^K} \sum_{i=1}^{2^K} \sum_{\substack{j=1 \\ \text{s.t. } b_1(H_i) \neq b_1(H_j)}}^{2^K} P_{H_i \rightarrow H_j} \triangleq P_U \quad (27)$$

$$P \geq \frac{1}{2^K} \sum_{\substack{i=1 \\ \mathbf{e}^{ij} = (b_1(H_i), 0, 0, \dots, 0)^T}}^{2^K} P_{H_i \rightarrow H_j} \triangleq P_L. \quad (28)$$

These bounds on error probability can be easily extended to the more general case of  $M$ -ary modulation and/or to the case where  $\mathcal{R}$  is not invertible. While the bounds in (28) can be numerically computed, the expressions for the pair-wise error probabilities are complicated and reveal no insight into the essential behavior of the error rate. This motivates the study of the asymptotic error rate as  $\sigma^2 \rightarrow 0$  in the rest of this paper. We restrict attention to the case of binary modulation.

## IV. ASYMPTOTIC BEHAVIOR OF ERROR PROBABILITY AS $\sigma^2 \rightarrow 0$

Notice that the pair-wise error rates depend on the values of  $c_{ij}$  and  $\lambda_{ij}^k$ . In Sections IV-A-D, we obtain the asymptotic low noise characterization of these quantities. Following that, we show that the error probability is asymptotically dominated by the unity-weight error vectors, which allows us to show that  $P_U$  and  $P_L$  are asymptotically coincident. This also yields an exact formula for asymptotic efficiency. In the rest of this paper, we will write the limit  $\sigma^2 \rightarrow 0$  equivalently as  $\gamma \rightarrow \infty$  with the energies of all users (and hence, the energy ratios) fixed.

### A. Asymptotics of $c_{ij}$

We first obtain the limit of  $c_{ij}$  defined in (20) as  $\gamma \rightarrow \infty$ . Note that for any hypothesis  $H_i$ ,  $\det(\mathcal{K}_{\mathbf{z}|H_i})$  is a polynomial of degree  $LK$  in  $\gamma$ . The threshold  $c_{ij}$  is the ratio of two such determinants. Hence, the limit of  $c_{ij}$  as  $\gamma \rightarrow \infty$  is obtained as

$$\bar{c}_{ij} \triangleq \lim_{\gamma \rightarrow \infty} c_{ij} = \ln \left( \frac{a_{LK}(\det(\mathcal{K}_{\mathbf{z}|H_i}))}{a_{LK}(\det(\mathcal{K}_{\mathbf{z}|H_j}))} \right) \quad (29)$$

where  $a_{LK}(\det(\mathcal{K}_{\mathbf{z}|H_i}))$  is the coefficient of  $\gamma^{LK}$  in  $\det(\mathcal{K}_{\mathbf{z}|H_i})$ .

A closed-form expression for  $\bar{c}_{ij}$  defined in (29) can be obtained as follows. Note that if we assume  $\mathbf{b}(H_i)$  to have all entries equal to unity, the asymptotic approximation of the matrix  $\mathcal{K}_{\mathbf{z}|H_i}$  has the form shown in (30) at the bottom of the page, where  $\mathcal{Q}_{kl}$  is the  $(k, l)$ th submatrix (of dimension  $L \times L$ ) in a  $2K \times 2K$  equiblock partition of the matrix  $\mathcal{Q}$ . Note that  $\mathcal{Q}_{kl}$  has a striped structure in that  $\mathcal{Q}_{kl} = \mathbf{Q}_{kl} \otimes \mathbf{I}_S$ , where  $\mathbf{Q}_{kl}$  is the  $(k, l)$ th submatrix (of dimension  $L_w \times L_w$ ) in a  $2K \times 2K$  equiblock partition of the matrix  $\mathbf{Q} = \mathbf{R}^{-1}$ .

In general (for any hypothesis), one can identify the block permutation matrix that will rearrange the elements of the asymptotic approximation of  $\mathcal{K}_{\mathbf{z}|H_i}$  into

$$\begin{pmatrix} \mathcal{K}_{\text{ul}}^{H_i} & \mathcal{K}_{\text{ur}}^{H_i} \\ \mathcal{K}_{\text{ll}}^{H_i} & \mathcal{K}_{\text{lr}}^{H_i} \end{pmatrix} \quad (31)$$

where the block diagonal elements of  $\mathcal{K}_{\text{ul}}^{H_i}$  are linearly proportional to  $\gamma$  [each of the submatrices in (31) is of dimension  $LK \times LK$ ]. Consequently, it can be shown, with some algebra, that

$$\begin{aligned} a_{LK}(\det(\mathcal{K}_{\mathbf{z}|H_i})) &= \det \left( \mathcal{K}_{\text{lr}}^{H_i} \right) a_{LK} \left( \det \left( \mathcal{K}_{\text{ul}}^{H_i} - \mathcal{K}_{\text{ur}}^{H_i} \times \left( \mathcal{K}_{\text{lr}}^{H_i} \right)^{-1} \mathcal{K}_{\text{ll}}^{H_i} \right) \right) \\ &= \det \left( \mathcal{K}_{\text{lr}}^{H_i} \right) \prod_{i=1}^K \det(r_i \Sigma_{ii}) \end{aligned} \quad (32)$$

$$= \det \left( \mathcal{K}_{\text{lr}}^{H_i} \right) \prod_{i=1}^K \det(r_i \Sigma_{ii}) \quad (33)$$

so that

$$\bar{c}_{ij} = \ln \left( \frac{\det \left( \mathcal{K}_{\text{lr}}^{H_i} \right)}{\det \left( \mathcal{K}_{\text{lr}}^{H_j} \right)} \right). \quad (34)$$

Notice that  $\bar{c}_{ij}$  is independent of the energy ratios  $\{r_k\}$  for any pair of hypotheses.

### B. Asymptotics of Eigenvalues

In this section, we study the asymptotic behavior of the eigenvalues of the matrix  $\mathcal{C}_{H_i H_j}$  that was defined in (22). We will first show that some of these eigenvalues are equal to zero for any SNR. To characterize the rest, we must consider the limiting behavior for high SNR.

For any two hypotheses  $H_i$  and  $H_j$ , the covariance matrices  $\mathcal{K}_{\mathbf{z}|H_i}$  and  $\mathcal{K}_{\mathbf{z}|H_j}$  can be permuted in a way that the elements corresponding to users indexed by all such  $k$  for which  $b_k(H_i) \neq b_k(H_j)$  are in the upper left corner, so that the permuted matrices (with a slight abuse of notation, we denote them by the same symbols)

$$\mathcal{K}_{\mathbf{z}|H_i} = \begin{pmatrix} \mathcal{K}_{11}^{H_i} & \mathcal{K}_{12} \\ \mathcal{K}_{12}^\dagger & \mathcal{K}_{22} \end{pmatrix} \quad \mathcal{K}_{\mathbf{z}|H_j} = \begin{pmatrix} \mathcal{K}_{11}^{H_j} & \mathcal{K}_{12} \\ \mathcal{K}_{12}^\dagger & \mathcal{K}_{22} \end{pmatrix}. \quad (35)$$

For an error vector with weight  $e$ , the matrix  $\mathcal{K}_{11}^{H_i}$  will be  $2Le \times 2Le$ . Using the fact that the second block row of the matrix  $\mathcal{K}_{\mathbf{z}|H_i} \mathcal{K}_{\mathbf{z}|H_j}^{-1}$  is equal to the second block row of the matrix  $\mathcal{K}_{\mathbf{z}|H_j} \mathcal{K}_{\mathbf{z}|H_i}^{-1}$  (which in turn is the identity matrix), it follows that the matrix  $\mathcal{C}_{H_i H_j}$  with the same partitioning as in (35) takes on the form  $\begin{pmatrix} (\mathcal{C}_{H_i H_j})_{11} & (\mathcal{C}_{H_i H_j})_{12} \\ \mathbf{0} & \mathbf{0} \end{pmatrix}$ , where the  $\mathbf{0}$ 's are all-zero matrices of appropriate dimensions. Thus, for an error vector of weight  $e$ ,  $2L(K - e)$  eigenvalues are equal to 0 and the nonzero eigenvalues coincide with those of  $(\mathcal{C}_{H_i H_j})_{11}$ . The key problem then is to analyze the asymptotic behavior of  $(\mathcal{C}_{H_i H_j})_{11}$ . A crucial step in this regard is to determine the inverse  $\mathcal{K}_{\mathbf{z}|H_i}^{-1}$  for high SNR.

The inverse of any  $N \times N$  invertible matrix  $\mathbf{M}$  can be computed as  $\mathbf{M}^{-1} = (\det(\mathbf{M}))^{-1} \mathbf{A}^T$ , with elements  $A_{kl} = (-1)^{k+l} \det(\mathbf{M}_{kl})$  where  $\mathbf{M}_{kl}$  is a matrix that results by striking out the  $k$ th row and  $l$ th column of  $\mathbf{M}$ .  $A_{kl}$  is called the *cofactor* of the matrix element  $M_{kl}$ . The matrix  $\mathbf{A}^T$  with entries  $A_{kl}$  as defined is called the *adjugate* of  $\mathbf{M}$  [14]. Whenever it is not clear from which matrix a cofactor is computed, we add it as an argument, as in  $A_{kl}(\mathbf{M})$ .

We introduce the notation  $\{N, \mathbf{X}\}$ , which means that each element in the  $L \times L$  polynomial matrix  $\mathbf{X}$  is of degree  $N$ . By applying the formula for the inverse to the matrix given in (30), and using the notation just described, we have (36), as shown at

$$\mathcal{K}_{\mathbf{z}|H_i} \approx \begin{pmatrix} \gamma \Sigma_{11} & \mathcal{Q}_{12} & \mathcal{Q}_{13} & \mathcal{Q}_{14} & \mathcal{Q}_{15} & \dots & \mathcal{Q}_{12K} \\ \mathcal{Q}_{12}^* & \mathcal{Q}_{22} & \mathcal{Q}_{23} & \mathcal{Q}_{24} & \mathcal{Q}_{25} & \dots & \mathcal{Q}_{22K} \\ \mathcal{Q}_{13}^* & \mathcal{Q}_{23}^* & r_2 \gamma \Sigma_{22} & \mathcal{Q}_{34} & \mathcal{Q}_{35} & \dots & \mathcal{Q}_{32K} \\ \mathcal{Q}_{14}^* & \cdot & \cdot & \mathcal{Q}_{44} & \cdot & \dots & \mathcal{Q}_{42K} \\ \mathcal{Q}_{15}^* & \cdot & \cdot & \cdot & r_3 \gamma \Sigma_{33} & \dots & \mathcal{Q}_{52K} \\ \vdots & \vdots & \vdots & \vdots & \vdots & \ddots & \vdots \\ \mathcal{Q}_{12K}^* & \cdot & \cdot & \cdot & \cdot & \dots & \mathcal{Q}_{2K2K} \end{pmatrix} \quad (30)$$

the bottom of the page, where the  $L \times L$  block entry (1,3), for example, of the transpose of the adjugate of  $\mathcal{K}_{\mathbf{z}|H_i}$  takes on the form

$$\left\{ LK - 2, \frac{1}{r_2} \begin{pmatrix} A_{12L+1} & A_{12L+2} & \dots & A_{13L} \\ A_{22L+1} & A_{22L+2} & \dots & A_{23L} \\ \vdots & \vdots & \ddots & \vdots \\ A_{L2L+1} & A_{L2L+2} & \dots & A_{L3L} \end{pmatrix} \right\} \quad (37)$$

where each entry  $A_{kl}$  in (37) is defined as  $A_{kl} = (-1)^{k+l} \det \left( \left( \mathcal{K}_{\mathbf{z}|H_i}^{eq} \right)_{kl} \right)$ .  $\mathcal{K}_{\mathbf{z}|H_i}^{eq}$  is defined as the covariance matrix of  $\mathbf{z}|H_i$  for equal energies among all users, i.e., as  $\mathcal{K}_{\mathbf{z}|H_i}$  with  $r_k = 1$  for all  $k$ . This notation is useful, because it enables us to explicitly recognize the dependence of the asymptotic form of the inverse of the matrix  $\mathcal{K}_{\mathbf{z}|H_i}$  on the energy ratios  $r_k$ . The common denominator polynomial denoted as  $\{LK, D_i\}$  in (36) is, of course,  $\det \left( \mathcal{K}_{\mathbf{z}|H_i}^{eq} \right)$ .

In general, the order of the polynomial elements of an  $L \times L$  block entry  $(k, l)$  of the adjugate of  $\mathcal{K}_{\mathbf{z}|H_i}^{eq}$  is as follows.

- $LK$ , if  $\left( \mathcal{K}_{\mathbf{z}|H_i}^{eq} \right)_{kk} \neq \gamma \Sigma_{kk}$  and  $\left( \mathcal{K}_{\mathbf{z}|H_i}^{eq} \right)_{ll} \neq \gamma \Sigma_{ll}$ .
- $LK - 1$ , if  $\left( \mathcal{K}_{\mathbf{z}|H_i}^{eq} \right)_{kk} \neq \gamma \Sigma_{kk}$  xor  $\left( \mathcal{K}_{\mathbf{z}|H_i}^{eq} \right)_{ll} \neq \gamma \Sigma_{ll}$ .
- $LK - 2$ , if  $\left( \mathcal{K}_{\mathbf{z}|H_i}^{eq} \right)_{kk} = \gamma \Sigma_{kk}$  and  $\left( \mathcal{K}_{\mathbf{z}|H_i}^{eq} \right)_{ll} = \gamma \Sigma_{ll}$

where we used XOR to denote a logic-exclusive OR.

With this insight, we investigate the asymptotic behavior of the matrix  $(\mathcal{C}_{H_i H_j})_{11}$ , in whose eigenvalues we are interested. It can be shown that for the general case of an error weight  $e$  with  $e \in \{1, 2, \dots, K\}$ , the asymptotic approximation of the matrix  $(\mathcal{C}_{H_i H_j})_{11}$  is given by (38) at the bottom of the page, where a matrix entry  $\mathbf{0}$  implies that the matrix in its place has polynomial elements whose highest exponent of  $\gamma$  are no greater than  $-1$ . We also assumed that all  $e$  nonzero elements of  $\mathbf{e}$  are equal to  $-1$ . The matrices  $\mathbf{C}_{mn}$ , with  $m, n \in \{1, 2, \dots, e\}$  are constants that are all independent of  $\gamma$ .

We are interested in the characteristic polynomial  $c(\lambda) \triangleq \det(\lambda \mathbf{I} - (\mathcal{C}_{H_i H_j})_{11})$ . We use Laplace's expansion and retain only terms which will give coefficients that involve  $\gamma^{Le}$ , since only such terms matter in the asymptotic analysis. Thus, we obtain the characteristic polynomial shown in (39) at the bottom of the page, where the matrix  $\mathcal{P}$  is implicitly defined. From (39), it is easily seen that  $-1$  is an eigenvalue with multiplicity  $Le$ . The other  $Le$  eigenvalues are positive, which follows from viewing the  $Le \times Le$  matrix  $\mathcal{P}$ , as the product of the diagonal matrix  $\text{diag}(1/r_2, \dots, r_e) \otimes \mathbf{I}_L$ , the block diagonal matrix  $\text{diag}[\Sigma_{11}, \Sigma_{22}, \dots, \Sigma_{ee}]$ , and a principal submatrix of the asymptotic form of the positive definite

$$\mathcal{K}_{\mathbf{z}|H_i}^{-1} \sim \frac{1}{\{LK, D_i\}} \times \begin{pmatrix} \{LK - 1, \mathbf{A}_{11}\} & \{LK - 1, \mathbf{A}_{12}\} & \left\{LK - 2, \frac{1}{r_2} \mathbf{A}_{13}\right\} & \{LK - 1, \mathbf{A}_{14}\} & \dots & \{LK - 1, \mathbf{A}_{12K}\} \\ \{LK - 1, \mathbf{A}_{21}\} & \{LK, \mathbf{A}_{22}\} & \left\{LK - 1, \frac{1}{r_2} \mathbf{A}_{23}\right\} & \{LK, \mathbf{A}_{24}\} & \dots & \{LK, \mathbf{A}_{22K}\} \\ \left\{LK - 2, \frac{1}{r_2} \mathbf{A}_{31}\right\} & \left\{LK - 1, \frac{1}{r_2} \mathbf{A}_{32}\right\} & \left\{LK - 1, \frac{1}{r_2} \mathbf{A}_{33}\right\} & \left\{LK - 1, \frac{1}{r_2} \mathbf{A}_{34}\right\} & \dots & \left\{LK - 1, \frac{1}{r_2} \mathbf{A}_{32K}\right\} \\ \{LK - 1, \mathbf{A}_{41}\} & \{LK, \mathbf{A}_{42}\} & \left\{LK - 1, \frac{1}{r_2} \mathbf{A}_{43}\right\} & \{LK, \mathbf{A}_{44}\} & \dots & \{LK, \mathbf{A}_{42K}\} \\ \vdots & \vdots & \vdots & \vdots & \ddots & \vdots \\ \{LK - 1, \mathbf{A}_{2K1}\} & \{LK, \mathbf{A}_{2K2}\} & \left\{LK - 1, \frac{1}{r_2} \mathbf{A}_{2K3}\right\} & \{LK, \mathbf{A}_{2K4}\} & \dots & \{LK, \mathbf{A}_{2K2K}\} \end{pmatrix}^T \quad (36)$$

$$(\mathcal{C}_{H_i H_j})_{11} \approx \begin{pmatrix} -\mathbf{I} & \mathbf{C}_{11} & \mathbf{0} & \mathbf{C}_{12} & \mathbf{0} & \dots & \mathbf{C}_{1e} \\ \mathbf{C}_{21} & \gamma \Sigma_{11} \frac{a_{LK}(\mathbf{A}_{22})}{a_{LK}(D_j)} & \mathbf{C}_{22} & \gamma \Sigma_{11} \frac{a_{LK}(\mathbf{A}_{42})}{a_{LK}(D_j)} & \mathbf{C}_{23} & \dots & \gamma \Sigma_{11} \frac{a_{LK}(\mathbf{A}_{(2e)2})}{a_{LK}(D_j)} \\ \mathbf{0} & \mathbf{C}_{31} & \mathbf{I} & \mathbf{C}_{32} & \mathbf{0} & \dots & \mathbf{C}_{3e} \\ \vdots & \vdots & \vdots & \vdots & \vdots & \ddots & \vdots \\ \mathbf{C}_{(2e)1} & r_e \gamma \Sigma_{ee} \frac{a_{LK}(\mathbf{A}_{2(2e)})}{a_{LK}(D_j)} & \mathbf{C}_{(2e)2} & r_e \gamma \Sigma_{ee} \frac{a_{LK}(\mathbf{A}_{4(2e)})}{a_{LK}(D_j)} & \mathbf{C}_{(2e)3} & \dots & r_e \gamma \Sigma_{ee} \frac{a_{LK}(\mathbf{A}_{(2e)(2e)})}{a_{LK}(D_j)} \end{pmatrix} \quad (38)$$

$$c(\lambda) \approx (\lambda + 1)^{Le} \det \begin{pmatrix} \lambda \mathbf{I} - \gamma \Sigma_{11} \frac{a_{LK}(\mathbf{A}_{22})}{a_{LK}(D_j)} & -\gamma \Sigma_{11} \frac{a_{LK}(\mathbf{A}_{42})}{a_{LK}(D_j)} & \dots & -\gamma \Sigma_{11} \frac{a_{LK}(\mathbf{A}_{(2e)2})}{a_{LK}(D_j)} \\ -r_2 \gamma \Sigma_{22} \frac{a_{LK}(\mathbf{A}_{24})}{a_{LK}(D_j)} & \lambda \mathbf{I} - r_2 \gamma \Sigma_{22} \frac{a_{LK}(\mathbf{A}_{44})}{a_{LK}(D_j)} & \dots & -r_2 \gamma \Sigma_{22} \frac{a_{LK}(\mathbf{A}_{(2e)4})}{a_{LK}(D_j)} \\ \vdots & \vdots & \ddots & \vdots \\ -r_e \gamma \Sigma_{ee} \frac{a_{LK}(\mathbf{A}_{2(2e)})}{a_{LK}(D_j)} & -r_e \gamma \Sigma_{ee} \frac{a_{LK}(\mathbf{A}_{4(2e)})}{a_{LK}(D_j)} & \dots & \lambda \mathbf{I} - r_e \gamma \Sigma_{ee} \frac{a_{LK}(\mathbf{A}_{(2e)(2e)})}{a_{LK}(D_j)} \end{pmatrix} \triangleq (\lambda + 1)^{Le} \det(\lambda \mathbf{I} - \mathcal{P}) \quad (39)$$

matrix  $(\mathcal{K}_{\mathbf{z}|H_j}^{eq})^{-1}$ , which is, thus, also positive definite. The positivity of the eigenvalues of  $\mathcal{P}$  follow from Sylvester's law of inertia [14]. As every element of  $\mathcal{P}$  is proportional to  $\gamma$ , all eigenvalues are, hence, also proportional to  $\gamma$ . Moreover, these eigenvalues depend on the energy ratios  $r_2, \dots, r_e$ .

In general, then, we conclude that for any arbitrary error vector of weight  $e$  (by appropriately renumbering the users and their signals, and following the above argument for the particular case of the error vector with all nonzero elements equal to  $-1$ ), the eigenvalues of  $\mathcal{C}_{H_i H_j}$  always have the following structure for high SNR: there are  $Le$  eigenvalues equal to  $-1$ ,  $Le$  eigenvalues positive and proportional to  $\gamma$ , and  $2L(K - e)$  eigenvalues equal to 0. Moreover, the positive eigenvalues are a function of the energy ratios of the interfering users whose indices are the same as those of the nonzero elements of the error vector.

Consider the important example of a unity-weight error vector  $\mathbf{e}^{ij} = (-10 \dots 0)^T$ . For the asymptotic form of  $(\mathcal{C}_{H_i H_j})_{11}$ , we obtain (40), as shown at the bottom of the page, where the submatrices  $\mathbf{C}_1, \mathbf{C}_2$  do not depend on  $\gamma$ . In (40), we assumed that user 1 sends signal 1 and that it is erroneously detected as signal 2. From (40), we see that for a unity-weight error vector,  $L$  of the asymptotic eigenvalues are  $-1$ , and  $L$  are positive and linear in  $\gamma$ . Note also that the asymptotic eigenvalues for error-weight one are independent of the energy levels of the interferers.

### C. Asymptotic Error Probability

In this section, we obtain high SNR approximations for pair-wise error probabilities. Subsequently, we obtain an approximation of the overall error probability that is asymptotically tight.

Consider hypotheses  $H_i$  and  $H_j$  for which the error vector  $\mathbf{e}_{ij}$  has weight  $e$ . Let  $\{\alpha_{l_{ij}} \gamma\}_{l=1}^{eL}$  denote the  $eL$  asymptotic positive eigenvalues of the matrix  $\mathcal{C}_{H_i H_j}$ .

Given the form of the asymptotic eigenvalues that were deduced in Section IV-B, we obtain from (21) the following asymptotic characteristic function of the Hermitian form  $f_{ij}$ :

$$\begin{aligned} G_{f_{ij}}(s) &\approx \frac{(-\gamma)^{-eL} \prod_{l=1}^{eL} (\alpha_{l_{ij}})^{-1}}{(s-1)^{eL} \prod_{l=1}^{eL} \left(s + \frac{1}{\gamma \alpha_{l_{ij}}}\right)} \\ &= \sum_{l=1}^{eL} \frac{A_{l_{ij}}}{(s-1)^l} + \sum_{l=1}^{eL} \frac{B_{l_{ij}}}{s + \frac{1}{\gamma \alpha_{l_{ij}}}} \end{aligned} \quad (41)$$

where the second equality results from a partial fraction expansion assuming that the positive eigenvalues are distinct. The coefficients  $A_{l_{ij}}$  and  $B_{l_{ij}}$  can be expressed as

$$\begin{aligned} A_{l_{ij}} &= \frac{(-1)^{eL}}{(eL-l)! \gamma^{eL} \prod_{k=1}^{eL} \alpha_{k_{ij}}} \frac{d^{eL-l}}{ds^{eL-l}} \\ &\quad \times \left[ \frac{1}{\prod_{k=1}^{eL} \left(s + \frac{1}{\alpha_{k_{ij}} \gamma}\right)} \right]_{s=1} \end{aligned} \quad (42)$$

$$B_{l_{ij}} = \frac{\gamma^{eL-1}}{\alpha_{l_{ij}} \left(\gamma + \frac{1}{\alpha_{l_{ij}}}\right)^{eL} \prod_{\substack{k=1 \\ k \neq l}}^{eL} \left(1 - \frac{\alpha_{k_{ij}}}{\alpha_{l_{ij}}}\right)}. \quad (43)$$

From (42), it can be seen that all  $A_{l_{ij}}$ 's are proportional to  $\gamma^{-eL}$  for high  $\gamma$ .

We begin by noting that if the asymptotic threshold  $\bar{c}_{ij}$  is nonnegative, then  $\bar{c}_{ji}$  is negative, and vice versa [see (34)]. Hence, we will, without loss of generality, consider pairs of hypotheses for which  $\bar{c}_{ij} \geq 0$ . Computing the inverse Laplace transform of (41), and integrating the resulting pdf over appropriate ranges, we obtain for the pair-wise error probabilities  $P_{H_i \rightarrow H_j}$  and  $P_{H_j \rightarrow H_i}$

$$\begin{aligned} P_{H_i \rightarrow H_j} &\approx \sum_{l=1}^{eL} (-1)^l A_{l_{ij}} \\ &\quad + \sum_{l=1}^{eL} \frac{1 - \exp\left(-\frac{\bar{c}_{ij}}{\alpha_{l_{ij}} \gamma}\right)}{\left(1 + \frac{1}{\alpha_{l_{ij}} \gamma}\right)^{eL} \prod_{\substack{k=1 \\ k \neq l}}^{eL} \left(1 - \frac{\alpha_{k_{ij}}}{\alpha_{l_{ij}}}\right)} \\ &\triangleq \tilde{P}_{H_i \rightarrow H_j} \end{aligned} \quad (44)$$

$$\begin{aligned} P_{H_j \rightarrow H_i} &\approx -\exp(\bar{c}_{ji}) \sum_{l=1}^{eL} \frac{1}{(l-1)!} \\ &\quad \times A_{l_{ji}} \sum_{m=0}^{l-1} (-1)^m \frac{(l-1)! \bar{c}_{01}^{l-1-m}}{(l-1-m)!} \\ &\triangleq \tilde{P}_{H_j \rightarrow H_i}. \end{aligned} \quad (45)$$

One should note that the SNR enters (44) and (45) also through the coefficients  $A_{l_{ij}}$ , which are, as we have already mentioned, proportional to  $\gamma^{-eL}$  for high  $\gamma$ . Thus, the pair-wise error probability in (44) and (45) would also decrease like  $\gamma^{-eL}$ , if the second sum in (44) is also proportional to  $\gamma^{-eL}$ . That this is indeed true is shown in Appendices A and B. Hence, the conditional error probability corresponding to a unity weight error vector decreases as  $\gamma^{-L}$ , whereas for  $e > 1$  it decreases with a

$$(\mathcal{C}_{H_i H_j})_{11} \approx \left( \begin{array}{c} -\mathbf{I} \\ \mathbf{C}_2 \quad \gamma \boldsymbol{\Sigma}_{11} \frac{1}{a_{LK} (\det(\mathcal{K}_{\mathbf{z}|H_j}^{eq}))} \end{array} \left( \begin{array}{cccc} \mathbf{C}_1 & & & \\ a_{LK}(A_{L+1L+1}) & a_{LK}(A_{L+1L+2}^*) & \dots & a_{LK}(A_{L+1L+2L}^*) \\ a_{LK}(A_{L+1L+2}) & a_{LK}(A_{L+2L+2}) & \dots & a_{LK}(A_{L+1L+2L}^*) \\ \vdots & \vdots & \ddots & \vdots \\ a_{LK}(A_{L+1L+2L}) & a_{LK}(A_{L+2L+2L}) & \dots & a_{LK}(A_{2L+2L}) \end{array} \right) \right) \quad (40)$$

$\gamma^{-eL}$  dependence. Consequently, we have the important result that

$$\lim_{\gamma \rightarrow \infty} \frac{P_{(H_i \rightarrow H_j)_e}}{P_{(H_i \rightarrow H_j)_1}} = 0 \quad (46)$$

which establishes that each  $P_{H_i}$ , the error probability conditioned on hypothesis  $H_i$  being true, is dominated by the  $P_{H_i \rightarrow H_j}$  where  $H_j$  is the hypothesis that differs from  $H_i$  only for user 1. As a result, we have the asymptotically tight approximation of overall error probability

$$P_1(\gamma) = \frac{1}{2^K} \sum_{i=1}^{2^K} P_{H_i} \approx \frac{1}{2^K} \sum_{i \in \mathcal{E}} (P_{H_i \rightarrow H_j} + P_{H_j \rightarrow H_i}) \quad (47)$$

$$\approx \frac{1}{2^K} \sum_{i \in \mathcal{E}} (\tilde{P}_{H_i \rightarrow H_j} + \tilde{P}_{H_j \rightarrow H_i}) \triangleq \tilde{P}_1(\gamma) \quad (48)$$

with  $j$  s.t.  $\mathbf{e}_{ij} = (b_1(H_i), 0, \dots, 0)^T$  and where the set of indices  $\mathcal{E} \{1 \leq i \leq 2^K; \bar{c}_{ij} \geq 0\}$ . The asymptotic expressions for  $\tilde{P}_{H_i \rightarrow H_j}$  and  $\tilde{P}_{H_j \rightarrow H_i}$  are given in (44) and (45). Note that the resulting approximation is asymptotically tight for both the union upper bound as well as the lower bound, based on unity-weight error vectors. Hence, the above approximation  $\tilde{P}_1(\gamma)$  is asymptotically tight.

As a consequence of the fact that the asymptotic thresholds and eigenvalues are independent of the energy ratios for unity-weight error vectors, we have the result that the asymptotic approximation for the bit-error probability is independent of these quantities also. This result is significant in that the asymptotic performance of the optimum detector is invariant to changes in the energy levels of interfering users, and hence, there is no near-far problem.

#### D. Asymptotic Efficiency

In this section, we consider the problem of exactly quantifying the performance degradation due to the interfering users rather than the background noise. A performance measure which captures this idea is the *asymptotic efficiency* (cf. [6], [7], [11]), which for user 1, is defined as

$$\eta_1 = \sup \left\{ 0 \leq \delta \leq 1, \lim_{\gamma \rightarrow \infty} \frac{P_1(\gamma)}{P^S(\delta\gamma)} \leq 1 \right\} \quad (49)$$

where  $P_1(\gamma)$  is the error probability of user 1 for any detector in the multiuser channel, and  $P^S(\delta\gamma)$  is the minimum achievable error probability in a single-user channel where only user 1 is active with SNR  $\delta\gamma$ . The single-user scheme uses the two nonorthogonal signals of user 1 together with the noncoherent detector that is optimal for that single-user channel. An exact formula for the asymptotic efficiency of user 1 for the optimum multiuser detector can be obtained by replacing  $P_1(\gamma)$  in (49) with the asymptotically tight approximation  $\tilde{P}_1(\gamma)$  of its error probability as obtained in Section IV-C.

To arrive at a closed-form expression for asymptotic efficiency, we have to compute the limit

$$\begin{aligned} & \lim_{\gamma \rightarrow \infty} \frac{P_1(\gamma)}{P^S(\delta\gamma)} \\ &= \lim_{\gamma \rightarrow \infty} \frac{\tilde{P}_1(\gamma)}{P^S(\delta\gamma)} \\ &= \frac{1}{2^K} \sum_{i \in \mathcal{E}} (\tilde{P}_{H_i \rightarrow H_j} + \tilde{P}_{H_j \rightarrow H_i}) \\ &= \lim_{\gamma \rightarrow \infty} \frac{\sum_{j \text{ s.t. } \mathbf{e}_{ij} = (b_1(H_i)00\dots 0)^T} (\tilde{P}_{H_i \rightarrow H_j} + \tilde{P}_{H_j \rightarrow H_i})}{P^S(\delta\gamma)}. \end{aligned} \quad (50)$$

From (50), we see that we have to obtain an asymptotic expression for the error probability for the single-user case. This is, of course, a special case of the multiuser problem. The receiver observes  $L$  time translates of one of the two correlated signals of user 1. The signal correlation matrix in the single-user scenario is the upper left  $2L \times 2L$ -dimensional principal submatrix of  $\mathcal{R}$ , defined in (7). All the arguments that we used to arrive at asymptotic expressions for the error probability of the joint optimum detector apply for the single-user case as well. So, the asymptotic expressions for error probability of the single-user case can formally be written as the ones for the optimum detector (with  $e = 1$ ) in (44) and (45). To distinguish the parameters characterizing the error probabilities of the two detectors, we will denote the ones for the single-user detector with the superscript  $S$ .

From (42), it can be seen that each  $A_{l_{ij}}$  is proportional not only to  $\gamma^{-L}$ , but also to  $\prod_{l=1}^L 1/\alpha_{l_{ij}}$  for high  $\gamma$ . The remaining proportionality constant is independent of the error event, and will be denoted with  $a_l$ . Thus,  $A_{l_{ij}}$  can be written as  $A_{l_{ij}} = a_l \gamma^{-L} \prod_{l=1}^L 1/\alpha_{l_{ij}}$ . With this notation, the limit in (50) becomes (51), as shown at the bottom of the page, where the outer sum in the numerator represents the averaging of the  $2^{K-1}$

$$\lim_{\gamma \rightarrow \infty} \frac{P_1(\gamma)}{P^S(\delta\gamma)} = \frac{\frac{1}{2^{K-1}} \sum_{i \in \mathcal{E}} \left[ \frac{\sum_{l=1}^L (-1)^l a_l}{\prod_{l=1}^L \alpha_{l_{ij}}} + \lim_{\gamma \rightarrow \infty} \left[ \gamma^L \sum_{l=1}^L s_{l_{ij}} \right] + \frac{\exp(-\bar{c}_{ij})}{\prod_{l=1}^L \alpha_{l_{ij}}} \sum_{l=0}^{L-1} \frac{1}{l!} a_{l+1} \sum_{m=0}^l (-1)^{m+1} \frac{l! (-\bar{c}_{ij})^{l-m}}{(l-m)!} \right]}{\frac{\sum_{l=1}^L (-1)^l a_l}{\delta^L \prod_{l=1}^L \alpha_{l_{10}}^S} + \lim_{\gamma \rightarrow \infty} \left[ \gamma^L \sum_{l=1}^L s_l^S \right] + \frac{\exp(-\bar{c}_{01}^S)}{\delta^L \prod_{l=1}^L \alpha_{l_{10}}^S} \sum_{l=0}^{L-1} \frac{1}{l!} a_{l+1} \sum_{m=0}^l (-1)^{m+1} \frac{l! (-\bar{c}_{01}^S)^{l-m}}{(l-m)!}} \quad (51)$$

error-weight one conditional error probabilities  $2^{-1}(P_{H_i \rightarrow H_j} + P_{H_j \rightarrow H_i})$ , and

$$s_{l_{ij}} = \frac{1 - \exp\left(-\frac{\bar{c}_{ij}}{\alpha_{l_{ij}} \gamma}\right)}{\left(1 + \frac{1}{\alpha_{l_{ij}} \gamma}\right)^L \prod_{\substack{k=1 \\ k \neq l}}^L \left(1 - \frac{\alpha_{k_{ij}}}{\alpha_{l_{ij}}}\right)}$$

$$s_l^S = \frac{1 - \exp\left(-\frac{\bar{c}_{01}^S}{\alpha_{l_{01}}^S \delta \gamma}\right)}{\left(1 + \frac{1}{\alpha_{l_{01}}^S \delta \gamma}\right)^L \prod_{\substack{k=1 \\ k \neq l}}^L \left(1 - \frac{\alpha_{k_{01}}^S}{\alpha_{l_{01}}^S}\right)}. \quad (52)$$

It remains to evaluate the limits of the form  $\lim_{\gamma \rightarrow \infty} \left[ \gamma^L \sum_{l=1}^L s_l \right]$  in the numerator and denominator. This is performed in Appendix A. With the result obtained there, the final expression for the asymptotic efficiency  $\eta_1^{\text{opt}}$  becomes as shown in (53) at the bottom of the page, with

$$\rho_{ij} = \frac{C_L \sum_{l=1}^L \frac{(\alpha_{l_{ij}})^{-L}}{\prod_{\substack{k=1 \\ k \neq l}}^L \left(1 - \frac{\alpha_{k_{ij}}}{\alpha_{l_{ij}}}\right)}}{(-1)^L L!}$$

$$\rho^S = \frac{C_L^S \sum_{l=1}^L \frac{(\alpha_l^S)^{-L}}{\prod_{\substack{k=1 \\ k \neq l}}^L \left(1 - \frac{\alpha_k^S}{\alpha_l^S}\right)}}{(-1)^L L!} \quad (54)$$

where  $C_L$  ( $C_L^S$ ) is a polynomial in  $\bar{c}_{ij}$  ( $\bar{c}_{01}^S$ ) and is specified in Appendix A. In specifying the asymptotic efficiency, we assumed that  $\bar{c}_{01}^S \geq 0$ . The corresponding expression when  $\bar{c}_{01}^S < 0$  is obtained similarly.

In the expression for the asymptotic efficiency of the joint optimum detector, only error probabilities corresponding to error-weight one vectors are considered. As these are independent of the energy of the interfering users, the asymptotic efficiency does not depend on the energies of the interfering users. Thus, (53) is also the near-far resistance (defined as the worst-case asymptotic efficiency over  $\{r_k\}_{k=2}^K$ ).

## V. NUMERICAL RESULTS

The central result of this paper was the convergence of the upper and lower bounds on the error probability of the optimum detector for high SNR and the invariance of the high SNR error rate asymptote to the relative signal strengths of interfering users.

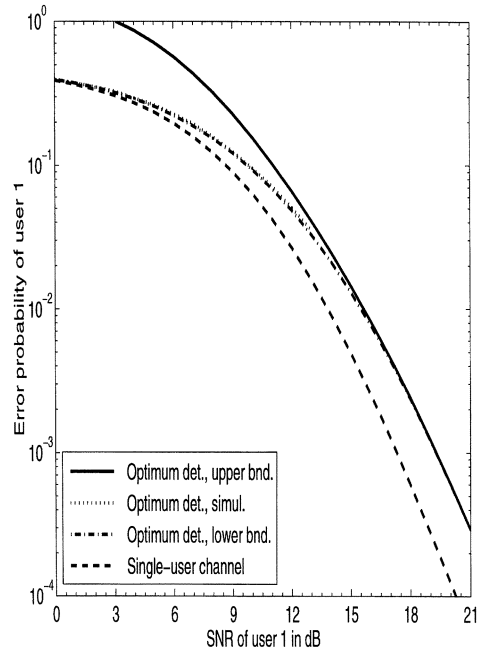


Fig. 1. Upper and lower bounds and simulations of error probability of the optimum detector for a four-path channel.

In this section, we illustrate these results for multipath diversity by considering a three-user channel, with the six signaling waveforms being Gold sequences of length 31. After the ISI mask, their effective length is  $32 - L$ . As the signal correlation matrix  $\mathcal{R}$  becomes singular for  $L > 4$ , and we limit our analysis to invertible correlation matrices, we take  $L \leq 4$ . Not only do we study the performance of the optimum detector as a function of diversity order  $L$ , but also as a function of the covariance matrices of the fading coefficients. In particular, two extreme cases are considered: one in which the  $L$  fading coefficients of each user are statistically independent, and the other in which they are fully correlated, i.e., each user's fading covariance matrix has entries that are all equal. The latter case effectively must result in a single-path performance (with diversity order 1), as the different paths contain the same information. In our examples, we also plot the error probability of the optimum detector of a single-user channel as a generally unachievable lower bound on error rate performance in a multiuser channel.

In Fig. 1, we depict the error probability of the joint optimum detector and the single-user channel optimum detector for four paths with equal strength and independent fading. Note that the

$$\eta_1^{\text{opt}} = \left( \frac{\sum_{l=1}^L \frac{(-1)^l a_l}{\prod_{i=1}^L \alpha_{i_{01}}^S} + \rho^S + \frac{\exp(-\bar{c}_{01}^S)}{\prod_{i=1}^L \alpha_{i_{01}}^S} \sum_{l=0}^{L-1} \frac{1}{l!} a_l \sum_{m=0}^l \frac{(-1)^{m+1} l! (-\bar{c}_{01}^S)^{l-m}}{(l-m)!}}{\sum_{i \in \mathcal{E}} \frac{1}{2^{k-1}} \left[ \frac{\sum_{l=1}^L \frac{(-1)^l a_l}{\prod_{i=1}^L \alpha_{i_{ij}}} + \rho_{ij} + \frac{\exp(-\bar{c}_{ij})}{\prod_{i=1}^L \alpha_{i_{ij}}} \sum_{l=0}^{L-1} \frac{1}{l!} a_l \sum_{m=0}^l \frac{(-1)^{m+1} l! (-\bar{c}_{ij})^{l-m}}{(l-m)!} \right]} \right)^{1/L} \quad (53)$$

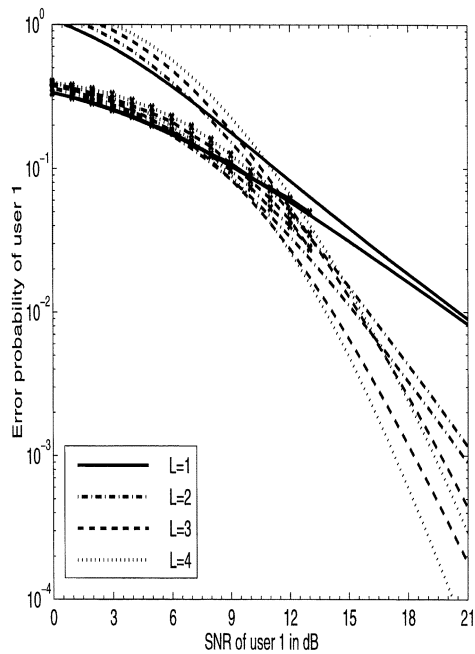


Fig. 2. Error probability of optimum multiuser detector (upper bound) and single-user detector (in a single-user channel) for different diversity orders (or multipath spreads).

TABLE I  
ASYMPTOTIC EFFICIENCY OF JOINT OPTIMUM DETECTOR  
FOR DIFFERENT MULTIPATH SPREADS

$L$	$\eta^J$
1	0.901
2	0.839
3	0.712
4	0.567

upper and lower bounds on error probability are asymptotically coincident, as they should be. The gap between single-user and multiuser performances implies here that the asymptotic efficiency of the optimum multiuser detector is strictly less than unity.

In Fig. 2, we plot the error rate of the joint optimum detector (upper bound) and the single-user channel optimum detector for the four cases  $L = 1, 2, 3, 4$  corresponding to different multipath spreads. The greater the multipath spread, the higher the order of diversity. Notice that the gap between the single-user detector and the multiuser detector increases as  $L$  increases. This is because the correlations between the  $3L$  signals increases with  $L$ , since the spread factor is kept nearly constant (the effective spread factor is just  $32 - L$  because of the ISI mask). This is reflected in the values for the asymptotic efficiency, depicted in Table I.

In Fig. 3, the error rates of the joint optimum detector (upper bound) and the single-user channel optimum detector are plotted for two cases. The first case corresponds to independent fading coefficients on the multiple paths of the same user's signals, i.e., each  $\Sigma_{kk}$  is diagonal. The second case is one where the fading coefficients for the same user's signals are fully correlated, i.e.,

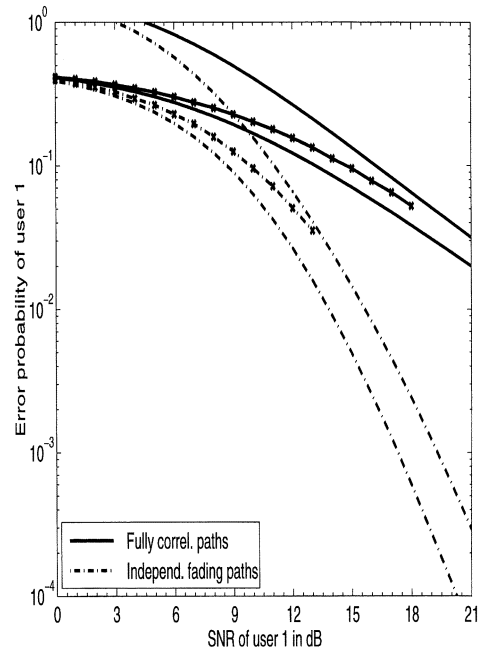


Fig. 3. Performance comparison of independently fading with fully correlated paths for optimum single and multiuser detectors (upper bound in the latter case), including simulated error rates for the multiuser case.

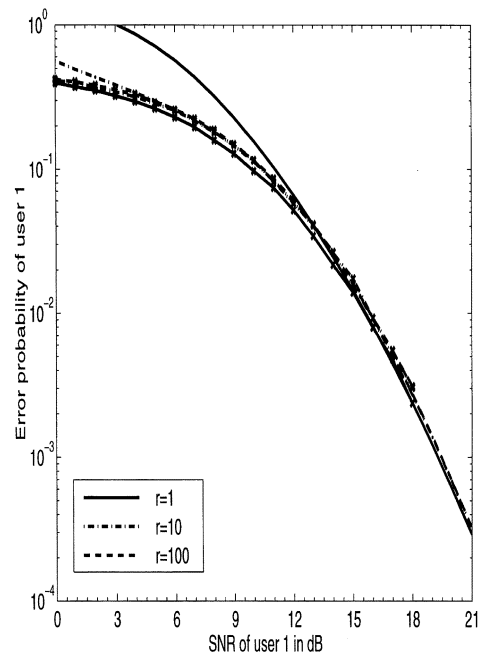


Fig. 4. Lower bound on and simulated error probability of optimum detector for various interferer energies.

each  $\Sigma_{kk}$  has all entries that are identical. Notice that the diversity order drops from four to one, as expected. The two cases of  $L = 1$  which are depicted in Fig. 2, and the fully correlated example of Fig. 3, are effectively the same and lead to almost the same performance. The slight performance difference is due to the ISI mask for the  $L = 4$  case.

Finally, we depict the interesting result that the high SNR error probability of the optimum detector for a particular user is effectively independent of the energies of the interfering users. This is illustrated in Fig. 4, where the error rate (lower bound)

is plotted for three cases where the ratio of interfering users to desired user signal strengths are equal to 1, 10, and 100, respectively. Notice that as the interfering signal strengths increase, the error rate bound decreases. This may seem contrary to what one might initially expect. However, such a result should not be surprising because with high interfering signal strengths, there is less uncertainty about those signals, which, in turn, implies that such signals are more effectively subtracted from the received signal by the optimum detector.

## VI. CONCLUSION

Optimum noncoherent multiuser detection for generalized multiuser diversity communications is studied. Upper and lower bounds on average error rate are obtained. The main focus of this paper was on deriving formulas for the asymptotic (high SNR) average bit-error probability of the optimum detector. It is shown that this asymptotic error rate for each user decays as the inverse of the  $L$ th power of the user's SNR, where  $L$  is the total diversity order (equal to the product of number of receive antennas and the order of transmit diversity). The single-user special case generalizes a result that is well known for an idealized single-user channel with independent and identical fading across diversity branches. Moreover, in the multiuser channel, it is shown that the asymptotic error rate is independent of the interfering signal strengths, and hence, that the optimum multiuser detector is near-far resistant. The performance of the optimum detector is also quantified in terms of an exact formula for its asymptotic efficiency, which is also equal to its near-far resistance.

## APPENDIX A

In this first appendix, we determine the limit

$$\rho \triangleq \lim_{x \rightarrow \infty} x^L \sum_{i=1}^L \frac{1 - \exp(-\frac{c}{\alpha_i x})}{\left( \prod_{\substack{j=1 \\ j \neq i}}^L \left(1 - \frac{\alpha_j}{\alpha_i}\right) \right) \left(1 + \frac{1}{\alpha_i x}\right)^L}. \quad (55)$$

Let us rewrite (55) in the following form:

$$\rho = \lim_{x \rightarrow \infty} \frac{\sum_{i=1}^L \frac{1 - \exp(-\frac{c}{\alpha_i x})}{\left( \prod_{\substack{j=1 \\ j \neq i}}^L \left(1 - \frac{\alpha_j}{\alpha_i}\right) \right) \left(1 + \frac{1}{\alpha_i x}\right)^L}}{\frac{1}{x^L}}. \quad (56)$$

We now apply l'Hospital's rule. After having computed the  $m$ th derivative, with  $m \leq L - 1$ , of both the numerator and denominator, we obtain the following indeterminate expression for  $\rho$ :

$$\rho = \frac{C_m \sum_{i=1}^L \frac{\alpha_i^{-m}}{\prod_{\substack{j=1 \\ j \neq i}}^L \left(1 - \frac{\alpha_j}{\alpha_i}\right)}}{(-1)^m \frac{L!}{(L-m)!} \lim_{x \rightarrow \infty} \frac{1}{x^{L-m}}} \quad (57)$$

where  $C_m$  is a polynomial in  $c$  and is independent of  $\alpha_i$ .

A sketch of the proof is as follows. The first derivative of the denominator of (56) gives  $-Lx^{-(L+1)}$ . The derivative of the

numerator will be proportional to  $x^{-2}$ , as both the derivative of  $1 + 1/\alpha_k x$  and  $\exp(-c/\alpha_k x)$  lead to such a dependence. Therefore, the  $x^{-2}$  in the numerator cancels with  $x^{-(L+1)}$  of the denominator, and the order in the exponent in the denominator reduces by one to  $L - 1$ . It is shown in Appendix B that the numerator in (57) is identically equal to zero for  $m = 1$  so that (57) is indeterminate. Taking the second derivatives of the numerator and the denominator of (56) yields (57) (with  $m = 2$ ), and again the numerator in (57) is identically equal to zero (for  $m = 2$ ), resulting in another indeterminate form for  $\rho$ . In fact, this continues until we take the  $(L - 1)$ th derivative, since terms in the numerator of (57) are equal to zero for each  $m \in \{1, 2, \dots, L - 1\}$ , as shown in Appendix B. Taking the  $L$ th derivative of the numerator and denominator in (56) and taking its limit as  $x \rightarrow \infty$  finally yields the desired limit

$$\rho = \frac{C_L \sum_{i=1}^L \frac{\alpha_i^{-L}}{\prod_{\substack{j=1 \\ j \neq i}}^L \left(1 - \frac{\alpha_j}{\alpha_i}\right)}}{(-1)^L L!}. \quad (58)$$

This limit is shown to be nonzero in Appendix B.

## APPENDIX B

In this appendix, we prove that, given a set of  $L$  positive and distinct numbers  $\{x_i\}_{i=1}^L$ , it is true that

$$\sum_{i=1}^L \frac{x_i^{L-l}}{\prod_{\substack{j=1 \\ j \neq i}}^L (x_i - x_j)} \triangleq \sum_{i=1}^L B_i \equiv 0 \quad (59)$$

for all  $l \in \{2, 3, \dots, L\}$ , whereas, it is nonzero for  $l = L + 1$ .

Let us define the function  $g(x)$

$$g(x) \triangleq \frac{x^{L-l}}{\prod_{i=1}^L (x - x_i)} \quad (60)$$

and perform a partial fraction expansion to get the equivalent expression

$$g(x) = \sum_{i=1}^L \frac{A_i}{x - x_i}, \quad \text{where } A_i = \frac{x_i^{L-l}}{\prod_{\substack{j=1 \\ j \neq i}}^L (x_i - x_j)}. \quad (61)$$

Note that  $A_i = B_i$ . If we now reconsider (61), and write it again with a common denominator, we obtain a third form for  $g(x)$

$$g(x) = \frac{\sum_{i=1}^L A_i \prod_{\substack{j=1 \\ j \neq i}}^L (x - x_j)}{\prod_{i=1}^L (x - x_i)}. \quad (62)$$

The coefficient of  $x^{L-1}$  in the numerator in (62), which is equal to  $\sum_{i=1}^L A_i$ , must be equal to zero because the coefficient of  $x^{L-1}$  in the numerator of (60) is zero for any  $l \in \{2, 3, \dots, L\}$ . This completes the proof.

To show that (59) is nonzero for  $l = L + 1$ , we proceed in an analogous way. The partial fraction expansion of  $g(x)$  now takes on the form

$$g(x) = \sum_{i=1}^L \frac{A_i}{x - x_i} + \frac{C}{x} \quad (63)$$

with

$$A_i = \frac{1}{x_i \prod_{\substack{j=1 \\ j \neq i}}^L (x_i - x_j)} \text{ and } C = \frac{(-1)^L}{\prod_{i=1}^L x_i}. \quad (64)$$

Now, writing (63) again with a common denominator, and using the property that the coefficient of  $x^L$  equals zero, results in the condition  $\sum_{i=1}^L A_i + C = 0$ , which implies that

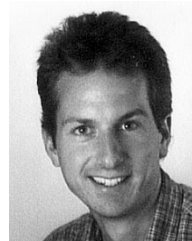
$$\sum_{i=1}^L \frac{x_i^{-l}}{\prod_{\substack{j=1 \\ j \neq i}}^L (x_i - x_j)} = -C \neq 0 \quad (65)$$

and proves the second part of our claim.

#### REFERENCES

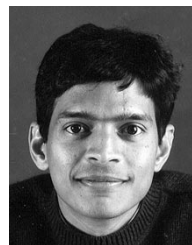
- [1] S. Vasudevan and M. K. Varanasi, "Achieving near-optimum asymptotic efficiency and fading resistance over the time-varying Rayleigh-faded CDMA channel," *IEEE Trans. Commun.*, vol. 44, pp. 1130–1143, Sept. 1996.
- [2] X. Wang and H. V. Poor, "Adaptive joint multiuser detection and channel estimation for multipath fading CDMA channels," *Wireless Networks*, vol. 4, no. 6, pp. 453–470, Nov. 1998.
- [3] M. K. Varanasi, "A systematic approach to the design and analysis of optimum DPSK receivers for generalized diversity communications over Rayleigh-fading channels," *IEEE Trans. Commun.*, vol. 47, pp. 1365–1375, Sept. 1999.
- [4] W. C. Jakes, *Microwave Mobile Communications*. New York: IEEE Press, 1993.
- [5] S. Verdú, "Minimum probability of error for asynchronous Gaussian multiple-access channels," *IEEE Trans. Inform. Theory*, vol. IT-32, pp. 85–96, Jan. 1986.
- [6] S. Verdú, "Optimum multiuser asymptotic efficiency," *IEEE Trans. Inform. Theory*, vol. IT-32, pp. 890–897, Sept. 1986.
- [7] Z. Zvonar and D. Brady, "Multiuser detection in single-path fading channels," *IEEE Trans. Commun.*, vol. 42, pp. 1729–1739, Feb.-Apr. 1994.

- [8] M. K. Varanasi and M. Brehler, "A systematic approach to noncoherent detection for DPSK modulation in multiuser correlated diversity Rayleigh-fading channels," in *Proc. Conf. Information Sciences and Systems*, Princeton, NJ, Mar. 1998, pp. 236–241.
- [9] A. Russ and M. K. Varanasi, "Noncoherent multiuser detection for nonlinear modulation over the Rayleigh-fading channel," *IEEE Trans. Inform. Theory*, vol. 47, pp. 295–307, Jan. 2001.
- [10] J. G. Proakis, *Digital Communication*, 3rd ed. New York: McGraw-Hill, 1995.
- [11] M. K. Varanasi, "Parallel group detection for synchronous CDMA communication over frequency-selective Rayleigh-fading channels," *IEEE Trans. Inform. Theory*, vol. 42, pp. 116–128, Jan. 1996.
- [12] R. Horn and C. Johnson, *Topics in Matrix Analysis*. Cambridge, U.K.: Cambridge Univ. Press, 1991.
- [13] M. Schwartz, W. Bennett, and S. Stein, *Communication Systems and Techniques*. New York: IEEE Press, 1996.
- [14] R. Horn and C. Johnson, *Matrix Analysis*. Cambridge, U.K.: Cambridge Univ. Press, 1985.



**Artur Russ** received the M.S. degree in electrical engineering from the University of Colorado, Boulder, in 1996, and the Dipl. Ing. degree in electrical engineering from the University of Erlangen-Nuremberg, Erlangen, Germany, in 1997.

He was a Research Associate at the University of Colorado until 1997, where his research activities were in the area of multiuser detection. In 1997, he joined Siemens Semiconductors, and later moved to Infineon Technologies, both in Munich, Germany. From 1999 to 2002 he was managing 2.5G/3G mixed-signal baseband chip development projects both in Munich and in Sophia-Antipolis, France. In 2002 he joined the BMW Group in Munich, and is currently involved in the development of driver assistance systems.



**Mahesh K. Varanasi** (S'87–M'89–SM'95) received the B.E. degree in electronics and communications engineering from Osmania University, Hyderabad, India in 1984, and the M.S. and Ph.D. degrees in electrical engineering from Rice University, Houston, TX, in 1987 and 1989, respectively.

In 1989, he joined the faculty of College of Engineering and Applied Sciences at the University of Colorado at Boulder, where he is currently Professor of Electrical and Computer Engineering. His teaching and research interests are in the areas of communication theory, information theory and signal processing. His research has been in multiuser detection, signal design and power control for multiple access, fading channels and diversity systems, blind receivers, and power and bandwidth-efficient multiuser communications and space-time communications.